Electron Transfer from Axial Ligand to S_1- and S_2-Excited Phosphorus Tetraphenylporphyrin

Mamoru Fujitsuka,[†] Dae Won Cho,[†,‡] Sachiko Tojo,[†] Azusa Inoue,[§] Tsutomu Shiragami,[§] Masahide Yasuda,[§] and Tetsuro Majima*[,†]

The Institute of Scientific and Industrial Research (SANKEN), Osaka University, Mihogaoka 8-1, Ibaraki, Osaka 567-0047, Japan, Department of Applied Chemistry, Faculty of Engineering, University of Miyazaki, Gakuen-Kibanadai, Miyazaki 889-2192, Japan, and Department of Chemistry, Chosun University, Gwangju 501-759, Korea

Received: August 6, 2007

Photoinduced processes of a series of phosphorus tetraphenylporphyrin (PTPP) derivatives ([PTPP-$(NHC_6H_4X)_2$]$^+Cl^-$, X = OCH_3, CH_3, H, Cl, CF_3, and CN) have been investigated by using femtosecond laser flash photolysis mainly. PTPP with OH as an axial ligand showed S_2 fluorescence upon excitation of the Soret band. The S_2 fluorescence lifetime was estimated to be 1.5 ps. On the other hand, both S_2 and S_1 fluorescence bands of PTPP−$(NHC_6H_4X)_2$ were difficult to observe, indicating the existence of an additional deactivation process such as charge separation (CS). From MO calculation and cyclic voltammetry, PTPP and the axial ligand are expected to act as an acceptor and a donor, respectively, upon excitation of PTPP. CS via the S_2 state was confirmed during the femtosecond laser flash photolysis by observing the transient absorption of radical anion of PTPP. Furthermore, CS via the S_1 state of PTPP was also observed. The CS rate via the S_1 state was faster than that from the S_2 state. The free energy dependence of the electron-transfer rates was discussed on the basis of Marcus theory.

Introduction

Nowadays, wide attention has been paid to light-energy conversion systems such as a solar cell sensitized by organic dyes.[1] To improve the efficiency of the device, employment of organic dye with a large absorption coefficient in a wide spectral range is essential. Usually, absorption spectra of organic dye comprise various transitions. Thus, photoabsorption generates various higher excited states as well as the lowest excited state. When an electron donor and an acceptor are located at close proximity, electron transfer occurs from the higher excited state before the relaxation to the lowest excited state.[2] Thus, the electron transfer from the higher excited state seems be an important subject to be cleared. However, the number of the studies on electron transfer from the higher excited state is rather limited, because of the quite short lifetime of these intermediates. Intermolecular electron transfer from S_2-excited zinc−tetraphenylporphyrin (ZnTPP) to solvent has been reported by Chosrowjan et al.[3a] Some intramolecular charge separation (CS) systems via the S_2 state using ZnTPP have been also reported.[3b−g] Recently, Mataga et al. have reported the systematic studies on the intramolecular CS process of S_2-excited zinc−porphyrin derivatives, in which an electron acceptor is attached at the meso-position of the porphyrin unit.[3d−f] Hayes et al. reported the substitution position dependence of the CS rate for S_2-excited ZnTPP derivatives.[3g] These results indicate that the higher excited state is an important intermediate in various photoinduced processes, including CS.

In the previous paper, we have investigated the CS and charge recombination (CR) processes of S_2-excited SbTPP derivatives, in which the donor was attached to SbTPP as an axial ligand, by using femtosecond spectroscopic measurements.[4] CS from the S_2 state was successfully observed for a part of the compounds, while that from the S_1 state was not confirmed. Thus, a detailed electron-transfer mechanism was not cleared.

In the present paper, we examined the CS and CR processes in PTPP derivatives (Figure 1). As in the case of SbTPP derivatives, an axial ligand of PTPP acts as an electron donor, indicating that the quite fast CS is possible because of the close proximity of donor and acceptor, even when the excited-state lifetime is quite short. From the investigation on the CS via the S_1 and S_2 states and CR processes, a wide range of driving force dependence of the electron-transfer rate can be examined. Such experiment is important, because one can elucidate characteristics of the electron transfer from the S_2 state, which may be different from that from the S_1 state.

Experimental Section

Materials. PTPP derivatives (**1a**−**f**) were synthesized as described in the Supporting Information. Compound **2** was synthesized according to a previously reported procedure.[5] All other chemicals were of the best commercial grades available.

Apparatus. The fluorescence lifetime in the sub-picosecond regime was measured using a fluorescence up-conversion method. The second harmonic oscillation (420 nm) of the output of the femtosecond laser (Spectra-Physics, Tsunami 3941-M1BB; full width at half-maximum (fwhm), 80 fs; 840 nm) pumped by a diode-pumped solid-state laser (Spectra-Physics, Millennia VIIIs) was used to excite the sample in a cell with a 1.0 mm optical path length. The residual fundamental and the

* To whom correspondence should be addressed. E-mail: majima@sanken.osaka-u.ac.jp.
[†] Osaka University.
[‡] Chosun University.
[§] University of Miyazaki.

10.1021/jp076303y CCC: $37.00
Published on Web 10/03/2007

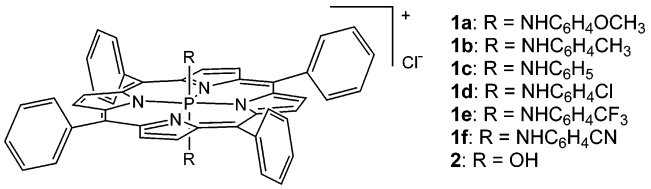

Figure 1. Molecular structure of PTPP derivatives in this study.

fluorescence were focused in a BBO type I crystal to generate a sum-frequency oscillation, which was detected by a photomultiplier tube (Hamamatsu Photonics, H8259) and a photon counter (Stanford Research Systems, SR400) after passing through a monochromator (Nikon G250). The cross-correlation time of the apparatus was 200 fs fwhm.

The sub-picosecond transient absorption spectra were measured by the pump and probe method using a regeneratively amplified titanium sapphire laser (Spectra Physics, Spitfire Pro F, 1 kHz) pumped by a Nd:YLF laser (Spectra Physics, Empower 15). The seed pulse was generated by the titanium sapphire laser mentioned above (800 nm). The second harmonic oscillation (400 nm, 130 fs fwhm, 8 μJ pulse^{-1}) of the output of the regeneratively amplified titanium sapphire laser was used as the excitation pulse. The excitation pulse at 550 nm was generated by optical parametric amplifier (Spectra Physics, OPA-800CF). A white light continuum pulse, which was generated by focusing the residual of the fundamental light to a flowing water cell after a computer-controlled optical delay, was divided into two parts and used as the probe and the reference lights, of which the latter was used to compensate the laser fluctuation. Both probe and reference lights were directed to a rotating sample cell with 1.0 mm of optical path and detected with a CCD detector equipped with a polychromator (Solar, MS3504). The pump pulse was chopped by a mechanical chopper synchronized to half of the laser repetition rate, resulting in a pair of spectra with and without the pump, from which the absorption change induced by the pump pulse was estimated.

Details of the pulse radiolysis are described in a previous paper.[6]

The steady-state absorption and fluorescence spectra were measured using a Shimadzu UV-3100PC and a Hitachi 850, respectively.

Electrochemical measurements were carried out in a conventional three-electrodes cell employing glassy carbon, platinum, and Ag/$AgNO_3$ electrodes as working, counter, and reference electrodes, respectively. The potential was scanned at 100 mV s^{-1} using a potentiostat. All electrochemical measurements were carried out with an acetonitrile solution containing 100 mM tetraethylammonium tetrafluoroborate after Ar bubbling.

Results and Discussion

Absorption and Fluorescence Spectra. Figure 2 shows absorption spectra of **2** and **1b**. Soret band and Q bands of **2** appeared at 423, 549, and 590 nm, respectively. On the other hand, those of **1b** were red-shifted to 429 and 568 nm, respectively. These shifts are attributable to the interaction with N atom of the axial ligand of PTPP.

Upon excitation of **2** at the Q band, fluorescence bands appeared at 607 and 658 nm. The fluorescence quantum yield was estimated to be 0.036, which is comparable to that of ZnTPP (0.04).[7] The fluorescence lifetime was 5.4 ns. On the other hand, upon excitation at 420 nm, which corresponds to the Soret band, the fluorescence peak was observed at 434 nm, indicating the

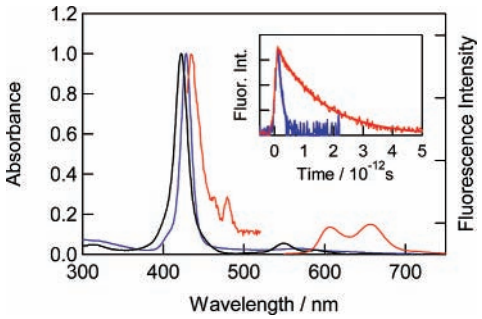

Figure 2. Normalized absorption spectra of **2** (black) and **1b** (blue) and fluorescence spectra of **2** (red) in acetonitrile. Inset: S_2 fluorescence decays of **2** (red) and **1b** (blue). Bold lines are fitted curves.

fluorescence from the S_2 state. Similar S_2 fluorescence has been reported for other metal-including TPPs.[8] By using the fluorescence up-conversion measurement, the decay profile of S_2 fluorescence was measured as indicated in the inset of Figure 2. The S_2 fluorescence of **2** decayed according to the single-exponential function with 6.5×10^{11} s^{-1} of the rate constant. Thus, the lifetime of the S_2 fluorescence of **2** in acetonitrile was estimated to be 1.5 ps. The estimated value is similar to SbTPP (2.0 ps)[4] but shorter than ZnTPP (3.5 ps).[3a]

In the case of **1b**, the fluorescence both from S_1 and S_2 states was difficult to observe. From the fluorescence up-conversion measurements, the S_2 fluorescence lifetime of **1b** was estimated to be 0.16 ps. The substantial decrease of the S_2 fluorescence lifetime indicates that a new process other than internal conversion is included by introducing the axial ligands including *N*-phenyl groups, which have electron-donating nature. As for the S_1 state of **1b**, the fluorescence lifetime was quite difficult to measure, because of low signal intensity. The absence of S_1 fluorescence also indicates the new deactivation pathway from the S_1-excited state. For other compounds, i.e., **1a** and **1c**−**f**, both S_1 and S_2 fluorescence bands were not observed. As the new deactivation pathway, electron transfer from the axial ligand to porphyrin ring is expected, because the axial ligand has an electron-donating nature.

MO and Redox Potentials. Figure 3 shows the energy minimized structure of **1b** at the B3LYP/3-21G* level.[9] PTPP has a distorted structure, because of the small radius of the included P atom. LUMO is localized on the TPP ring. HOMO is on the *N*-phenyl group. HOMO-1 is on another *N*-phenyl group of **1b**, which is energetically degenerated with HOMO. HOMO-2 of **1b** corresponds to HOMO of TPP ring. Thus, upon excitation of the TPP ring, electron transfer from HOMO of **1b**, i.e. the *N*-phenyl group, is expected. That is, PTPP and the *N*-phenyl ring are expected to act as an electron acceptor and a donor, respectively, in the electron transfer.

Table 1 summarizes the reduction potentials of **1a**−**f** as well as the oxidation potentials of the corresponding aniline derivatives estimated by cyclic voltammetry. The oxidation potentials of **1a**−**f** were difficult to measure because of instability upon oxidation. The oxidation potential varies according to the electron-donating or -accepting nature of the substituent group at the 4-position of the *N*-phenyl group. On the other hand, variation of the reduction potential is rather small. The reduction potential of the compounds corresponds to the reduction of the TPP ring, while the oxidation potential is attributable to that of the *N*-phenyl group.

From the oxidation and reduction potentials listed in Table 1, free energy changes for CS (ΔG_{CS}) upon S_1 and S_2 excitation were evaluated as listed in Table 1. For S_1 excitation, −0.22 to −0.76 eV of ΔG_{CS} are expected. For all compounds, CS is an

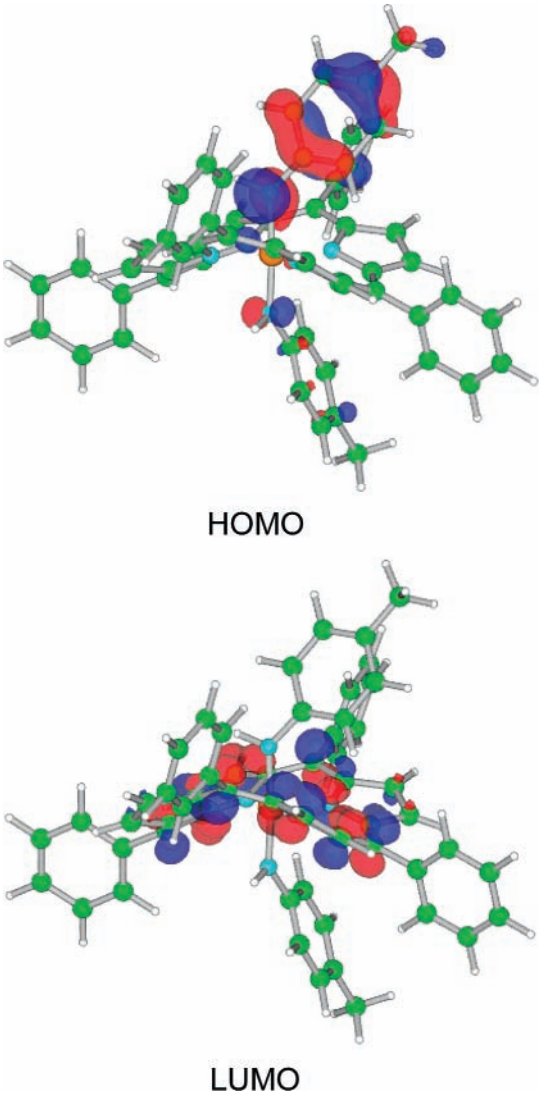

Figure 3. HOMO and LUMO of **1b** calculated at the B3LYP/3-21G* level.

exothermic process. Upon S_2 excitation, −1.58 to −1.04 eV of free energy change is expected. A larger free energy change for S_2 excitation can be attributed to the larger excitation energy of the S_2 state. Table 1 also listed the free energy changes for the CR process (ΔG_{CR}), which are slightly larger than the ΔG_{CS} values from the S_2 state. Thus, by estimating these rate constants, a relatively wide range of free energy change dependence of the electron-transfer rate can be examined.

Radical Anion of PTPP. As discussed in the above sections, the PTPP ring is expected to act as an electron acceptor upon photoexcitation of the PTPP ring. To confirm CS upon excitation, observation of the radical anion of PTPP is essential, although the absorption spectrum of the radical anion of PTPP has not been reported. Thus, we tried to observe the radical anion of PTPP by transient absorption measurement during the pulse radiolysis, because the reducing agent generated during the pulse radiolysis is quite strong. Figure 4 shows the transient absorption spectra of **2** in dimethylformamide (DMF) obtained during the pulse radiolysis. Immediately after the electron pulse irradiation, the transient absorption showed quite broad absorption attributable to solvated electron in DMF. At 5 μs after the electron pulse, the absorption band showed a peak around 690 nm, which can be assigned to the radical anion of PTPP, which is generated by capturing an electron from the solvent.

Although the report on the radical anion of TPP is limited, the observed radical anion of PTPP is quite similar to that of SbTPP, which shows absorption around 710 nm.[4,10] Thus, the present absorption change would be a common spectral feature for the radical anion of TPP.

Electron Transfer from the S_2 State. The photoinduced process upon excitation to the S_2 state of PTPP was examined by measuring the transient absorption spectra during the laser flash photolysis using a femtosecond laser at 400 nm. Figure 5 shows transient absorption spectra of **1b** in acetonitrile during the laser flash photolysis. Upon excitation, a transient absorption peak appeared at 700 nm with $(0.15\ \text{ps})^{-1}$ of rate constant, with the ground-state bleaching at 565 nm. The absorption band around 700 nm indicates the generation of radical anion of PTPP, that is, the charge-separated state of **1b**, because the observed peak agreed well with that observed during the pulse radiolysis (Figure 4). The observed spectral shape is quite different from that of the excited state of PTPP, which is shown in the Supporting Information. Furthermore, the generation rate agreed well with the S_2 fluorescence decay rate indicated in the above section. These results indicate that CS occurred from the S_2 state,

$$[\text{PTPP}(\text{NHC}_6\text{H}_4\text{CH}_3)]^+(S_2)-\text{NHC}_6\text{H}_4\text{CH}_3 \rightarrow [\text{PTPP}(\text{NHC}_6\text{H}_4\text{CH}_3)]^{\bullet}-(\text{NHC}_6\text{H}_4\text{CH}_3)^{\bullet+} \quad (1)$$

The rate constant of CS from the S_2 state (k_{CS_2}) was estimated according to

$$k_{CS_2} = k_{obs} - 1/\tau_{S_2,\mathbf{2}} \quad (2)$$

where k_{obs} and $\tau_{S_2,\mathbf{2}}$ are the observed generation rate of the radical anion of PTPP and the S_2 fluorescence lifetime of **2**, respectively, based on the assumption that the internal conversion rate and radiative rate of the S_2-excited-state of **1a**−**f** are the same as those of **2**. Furthermore, the quantum yield for CS from the S_2 state (Φ_{CS_2}) was estimated by

$$\Phi_{CS_2} = k_{CS_2}/k_{obs} \quad (3)$$

The estimated k_{CS_2} and Φ_{CS_2} values are listed in Table 2. The formation of the CS state from the S_2 state was also confirmed for **1a** and **1c**−**f** in acetonitrile. Except for **1e**, the CS from the S_2 state is a rather efficient pathway. The present fast CS from the ligand can be attributed to high electron density at N of the ligand in HOMO. The close proximity of the portion with high electron density in HOMO to the PTPP enables the fast CS via the S_2 state in spite of a quite short S_2 lifetime.

The generated radical ion pair decayed according to the single-exponential function. After the decay of the charge-separated state, transient absorption attributable to other species was not confirmed. Thus, it was indicated that, after the CS, the generated charge-separated state decayed to the ground state by CR. The CR rate (k_{CR_2}) was summarized in Table 2. The lifetime of the charge separated state was 0.52−4.8 ps.

Electron Transfer from the S_1 State. By using the 550 nm femtosecond laser pulse, the photoinduced process from the S_1 state of PTPP derivatives was investigated. Figure 6 is the transient absorption spectra of **1b** obtained during the laser flash photolysis using the 550 nm laser pulse, which excites at the Q-band of PTPP. Upon excitation, **1b** shows a transient absorption band attributable to the radical anion of PTPP at 700 nm. It is notable that the radical anion appeared quite rapidly within almost the pulse duration of the excitation laser (∼100

TABLE 1: Oxidation and Reduction Potentials and Free Energy Changes for Charge Separation and Recombination of PTPP Derivatives ($[PTPP-(NHC_6H_4X)_2]^+Cl^-$)

	X	$E_{ox.}$ [a,b]/V	$E_{red.}$ [a]/V	$-\Delta G_{CS_1}$ [c]/eV	$-\Delta G_{CS_2}$ [c]/eV	$-\Delta G_{CR}$/eV
1a	OCH_3	0.34	−0.94	0.76	1.58	1.28
1b	CH_3	0.52	−0.92	0.60	1.42	1.46
1c	H	0.68	−0.91	0.45	1.27	1.59
1d	Cl	0.72	−0.86	0.46	1.28	1.58
1e	CF_3	1.00	−0.82	0.22	1.04	1.82
1f	CN	1.03	−0.74	0.27	1.09	1.77

[a] V vs Ag^+/Ag. [b] Oxidation potential of corresponding aniline derivatives. [c] ΔG_{CS} values are estimated using $\Delta G_{CS} = E_{ox.} - E_{red.} - E_0$, where E_0 is excitation energy. As S_1 and S_2 energies, those of **2** (2.04 and 2.86 eV, respectively) were employed, because of the absence of S_1 and S_2 fluorescence of **1a**−**f**. Subscripts 1 and 2 of free energy changes denote the S_1 and S_2 excitation, respectively.

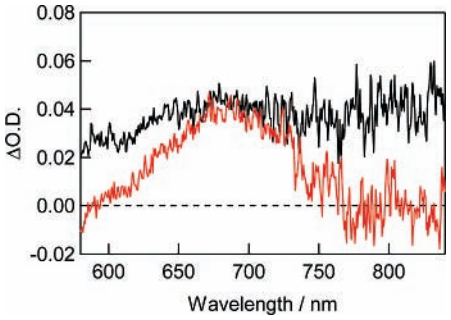

Figure 4. Transient absorption spectra of **2** in DMF during the pulse radiolysis. The black and red lines are the spectra at 0 ns and 5 μs after the electron pulse, respectively.

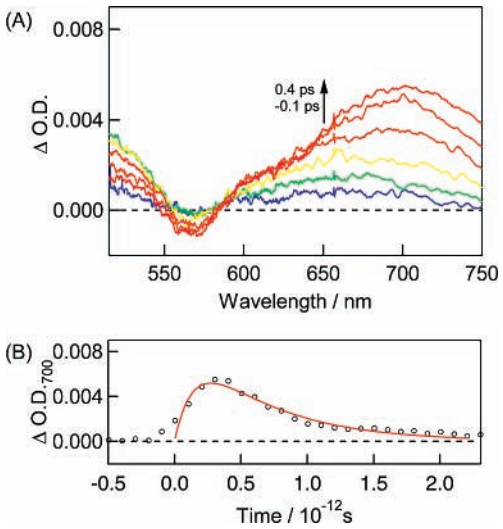

Figure 5. (A) Transient absorption spectra at −0.1, 0, 0.1, 0.2, 0.3, and 0.4 ps of **1b** in acetonitrile during the laser flash photolysis using 400 nm laser pulse (fwhm, 100 fs). (B) Kinetic trace of ΔOD at 700 nm during the laser flash photolysis.

fs). For comparison, kinetic traces of ΔOD at 700 nm upon S_2 and S_1 excitation are indicated in Figure 6B. This result indicates faster CS from the S_1 state than that from the S_2 state. Quite fast CS from the S_1 state was also confirmed with other PTPP derivatives. The rate constant (k_{CS_1}) and quantum yield (Φ_{CS_1}) for the CS via the S_1 state were estimated by manners similar to those in eqs 2 and 3, respectively. Because of the quite fast CS, the Φ_{CS_1} is unity for all compounds.

After the CS, the charge-separated state showed decay due to CR generating the corresponding ground state. k_{CR_1} was summarized in Table 2. The k_{CR_1} values are essentially the same as the k_{CR_2} values.

Free Energy Change Dependence of Electron-Transfer Rate. The observed electron-transfer rates, i.e., k_{CS} and k_{CR},

TABLE 2: Charge Separation (k_{CS_1} and k_{CS_2}) and Recombination (k_{CR_1} and k_{CR_2}) Rate Constants of PTPP Derivatives Observed by S_1 and S_2 Excitations[a]

	$10^{-12}k_{CS_1}$ [b]/s^{-1}	$10^{-12}k_{CR_1}$/s^{-1}	$10^{-12}k_{CS_2}$ [b]/s^{-1}	$10^{-12}k_{CR_1}$/s^{-1}
1a	13 (1.0)	2.6	6.4 (0.90)	1.9
1b	7.9 (1.0)	2.1	6.1 (0.90)	1.7
1c	14 (1.0)	0.57	3.5 (0.83)	0.70
1d	9.3 (1.0)	0.93	4.0 (0.83)	1.2
1e	10 (1.0)	0.21	1.0 (0.59)	0.24
1f	7.3 (1.0)	0.25	3.5 (0.83)	0.21

[a] Subscripts 1 and 2 of rate constants denote the S_1 and S_2 excitation, respectively. [b] Numbers in parentheses are quantum yields for charge separation (Φ_{CS_1} and Φ_{CS_2}).

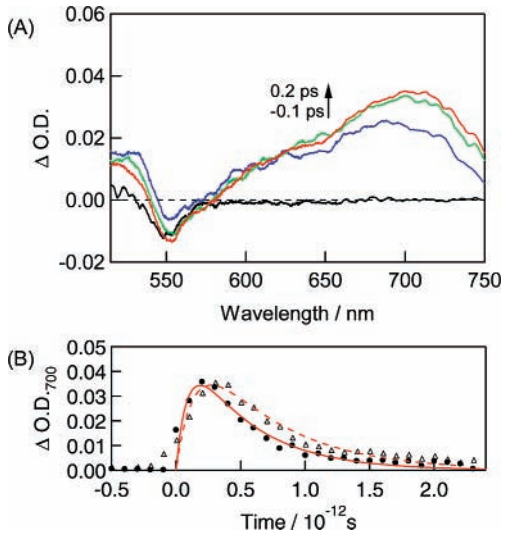

Figure 6. (A) Transient absorption spectra at −0.1, 0, 0.1, and 0.2 ps of **1b** in acetonitrile during the laser flash photolysis using 550 nm laser pulse (fwhm, 100 fs). (B) Kinetic trace of ΔOD at 700 nm during the laser flash photolysis. Triangles indicate the kinetic trace obtained by 400 nm excitation.

are discussed on the basis of the Marcus theory.[11] In Figure 7, the observed electron-transfer rates are plotted against the free energy changes. Usually, the electron-transfer rate depends on the free energy change according to

$$k_{ET} = \sqrt{\frac{\pi}{\hbar^2 \lambda_S k_B T}} |V|^2 \sum_m (e^{-S}(S^m/m!)) \times \exp\left(-\frac{(\lambda_S + \Delta G + m\hbar\langle\omega\rangle)^2}{4\lambda_S k_B T}\right) \quad (4)$$

$$\lambda_S = e^2\left(\frac{1}{2r_D} + \frac{1}{2r_A} - \frac{1}{r}\right)\left(\frac{1}{n^2} - \frac{1}{\epsilon_S}\right) \quad (5)$$

$$S = \frac{\lambda_V}{\hbar\langle\omega\rangle} \quad (6)$$

In eq 4, λ_S is the solvent reorganization energy given by eq 5, V is the electronic coupling, S is the electron-vibration coupling constant given by eq 6, $\langle\omega\rangle$ is the averaged angular frequency. In eq 5, r_D, r_A, r, and n are donor radius, acceptor radius, center-to-center distance, and refractive index, respectively. In eq 6, λ_V is the internal reorganization energy. From Figure 3, the r_D, r_A, and r values were estimated to be 2.1, 4.2, and 3.0 Å, respectively. Using these values, the λ_S value was estimated to be 0.18 eV. In Figure 7, eq 4 was calculated as a red line by assuming λ_V, V, and $\hbar\langle\omega\rangle$ are to be 0.57, 0.035, and 0.15 eV, respectively. The calculated curve well-reproduced the k_{CS_1}, k_{CR_1}, and k_{CR_2} values. That is, CS from the S_1 state is in the top region, while CRs in the inverted region. On the other hand, although the k_{CS_2} values are located at close position to the red line, k_{CS_2} values become larger as the $-\Delta G_{CS}$ value increases, indicating that the k_{CS_2} values are in the normal region of another parabola. This fact suggests that the total reorganization energy for CS from the S_2 state is larger than that from the S_1 state, probably because of a difference in molecular structure in the S_1 and S_2 states, which causes a difference in the λ_V value. The large difference in the λ_S value cannot be expected. In Figure 7, the blue curve was obtained by just changing the λ_V value to be 1.65 eV, while other parameters are the same as the red line. The good fit supports the above consideration.

As indicated in the Introduction, the papers on the electron transfer from the S_2 state of porphyrins are limited.[3] Mataga et al. investigated free energy change dependence of the electron-transfer rate from the S_2-excited zinc porphyrin derivatives, in which zinc porphyrin acts as an electron donor.[3d−f] They showed that the observed electron-transfer rates were well-reproduced by the Marcus theory assuming 0.3 eV of λ_V, which is much smaller than the value employed in this study. Although they have not examined CS from the S_1 state of the same compounds, the λ_V values for electron transfer from the various S_1-excited zinc porphyrin derivatives have been reported to be 0.3−0.6 V,[12] which is similar to the λ_V for electron transfer from the S_2 state reported by Mataga et al. Thus, the zinc porphyrin derivatives, which have a planar structure, do not have large structural differences between the S_1 and S_2 states. On the other hand, the present PTPP derivatives have a distorted structure in the ground state, as indicated in Figure 3. The excited PTPP possibly takes different structures depending on the excited state from the ground state, in order to reduce instability in the excited state. Such structural change causes the difference in the λ_V values.

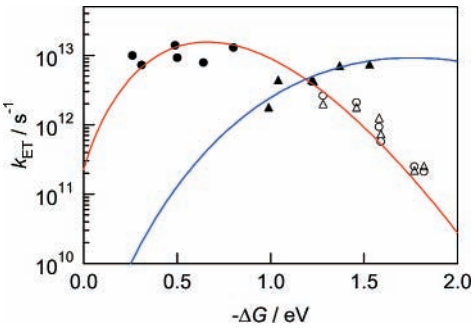

Figure 7. Free energy change ($-\Delta G$) dependence of the electron-transfer rate (k_{ET}, i.e., k_{CS} (filled mark) and k_{CR} (opened mark)) of PTPP derivatives upon excitation to S_1 (circle) and S_2 (triangle) states. Solid lines were calculated using eq 4 in the text by assuming $\lambda_S = 0.18$ eV, $V = 0.035$ eV, $\hbar\langle\omega\rangle = 0.15$ eV, and $\lambda_V = 0.57$ eV for S_1 excitation (red line) and 1.65 eV for S_2 excitation (blue line).

Estimation of the molecular geometry in the excited state is a quite difficult task both in the experimental and theoretical methods. Although we tried to estimate the molecular geometry in the excited states by using theoretical calculation, these attempts failed, even for simplified molecular structures. The reliable calculation of the large molecule in the higher excited states will be a future target. Still, the present experimental results indicate that the electron transfer in the higher excited state should be treated by a different manner from that from the lowest excited state.

Conclusion

Upon excitation of the Soret band of the PTPP derivatives, the charge-separated state was generated efficiently in spite of the quite short lifetime of the S_2 state. Efficient CS can be attributed to the high electron density of the N atom of the ligand. The CS rate via the S_1 state was faster than that from the S_2 state. Furthermore, the CS rate from the S_2 state was explained on the basis of a different λ_V value from that of the S_1 state. This result possibly indicates a different molecular structure in the S_2 state from that in the S_1 state.

Acknowledgment. We thank the members of the Radiation Laboratory of ISIR, Osaka University, for running the linear accelerator. This work has been partly supported by a Grant-in-Aid for Scientific Research (Projects 17105005, 19350069, and others) from the Ministry of Education, Culture, Sports, Science and Technology (MEXT) of the Japanese Government.

Supporting Information Available: Synthesis of **1a**−**f** and transient absorption spectrum of **2** in acetonitrile. These materials are available free of charge via the Internet at http://pubs.acs.org.

References and Notes

(1) For example; (a) O'Regan, B.; Graetzel, M. *Nature* **1991**, *353*, 737. (b) Hagfeldt, A.; Graetzel, M. *Acc. Chem. Res.* **2000**, *33*, 269.

(2) (a) Lenzmann, F.; Krueger, J.; Burnside, S.; Brooks, K.; Graetzel, M.; Gal, D.; Ruehle, S.; Cahen, D. *J. Phys. Chem. B* **2001**, *105*, 6347. (b) Huber, R.; Moser, J. E.; Graetzel, M.; Wachtveitl, J. *J. Phys. Chem. B* **2002**, *106*, 6494. (c) Pelet, S.; Graetzel, M.; Moser, J.-E. *J. Phys. Chem. B* **2003**, *107*, 3215.

(3) (a) Chosrowjan, H.; Taniguchi, S.; Okada, T.; Takagi, S.; Arai, T.; Tokumaru, K. *Chem. Phys. Lett.* **1995**, *242*, 644. (b) LeGourrérec, D.; Andersson, M.; Davidsson, J.; Mukhtar, E.; Sun, L.; Hammarström, L. *J. Phys. Chem. A* **1999**, *103*, 558. (c) Andersson, M.; Davidsson, J.; Hammarström, L.; Korppi-Tommola, J.; Peltola, T. *J. Phys. Chem. B* **1999**, *103*, 3258. (d) Mataga, N.; Chosrowjan, H.; Shibata, Y.; Yoshida, N.; Osuka, A.; Kikuzawa, T.; Okada, T. *J. Am. Chem. Soc.* **2001**, *123*, 12422. (e) Mataga, N.; Chosrowjan, H.; Taniguchi, S.; Shibata, Y.; Yoshida, N.; Osuka, A.; Kikuzawa, T.; Okada, T. *J. Phys. Chem. A* **2002**, *106*, 12191. (f) Mataga, N.; Taniguchi, S.; Chosrowjan, H.; Osuka, A.; Yoshida, N. *Chem. Phys.* **2003**, *295*, 215. (g) Hayes, R. T.; Walsh, C. J.; Wasielewski, M. R. *J. Phys. Chem. A* **2004**, *108*, 2375.

(4) Fujitsuka, M.; Cho, D. W.; Shiragami, T.; Yasuda, M.; Majima, T. *J. Phys. Chem. B* **2006**, *110*, 9368.

(5) (a) Kunimoto, K.; Segawa, H.; Shimidzu, T. *Tetrahedron Lett.* **1992**, *33*, 6327. (b) Andou, Y.; Ishikawa, K.; Shima, K.; Shiragami, T.; Yasuda, M.; Inoue, H. *Bull. Chem. Soc. Jpn.* **2002**, *75*, 1757.

(6) Fujitsuka, M.; Cho, D. W.; Tojo, S.; Yamashiro, S.; Shinmyozu, T.; Majima, T. *J. Phys. Chem. A* **2006**, *110*, 5735.

(7) Murov, S. L.; Carmichael, I.; Hug, G. L. *Handbook of Photochemistry*, 2nd ed.; Dekker: New York, 1993.

(8) As a review: Tokumaru, K. *J. Porphorins Phthalocyanines* **2001**, *5*, 77.

(9) Frisch, M. J.; Trucks, G. W.; Schlegel, H. B.; Scuseria, G. E.; Robb, M. A.; Cheeseman, J. R.; Montgomery, J. A., Jr.; Vreven, T.; Kudin, K. N.; Burant, J. C.; Millam, J. M.; Iyengar, S. S.; Tomasi, J.; Barone, V.; Mennucci, B.; Cossi, M.; Scalmani, G.; Rega, N.; Petersson, G. A.; Nakatsuji, H.; Hada, M.; Ehara, M.; Toyota, K.; Fukuda, R.; Hasegawa, J.; Ishida, M.; Nakajima, T.; Honda, Y.; Kitao, O.; Nakai, H.; Klene, M.; Li,

X.; Knox, J. E.; Hratchian, H. P.; Cross, J. B.; Bakken, V.; Adamo, C.; Jaramillo, J.; Gomperts, R.; Stratmann, R. E.; Yazyev, O.; Austin, A. J.; Cammi, R.; Pomelli, C.; Ochterski, J. W.; Ayala, P. Y.; Morokuma, K.; Voth, G. A.; Salvador, P.; Dannenberg, J. J.; Zakrzewski, V. G.; Dapprich, S.; Daniels, A. D.; Strain, M. C.; Farkas, O.; Malick, D. K.; Rabuck, A. D.; Raghavachari, K.; Foresman, J. B.; Ortiz, J. V.; Cui, Q.; Baboul, A. G.; Clifford, S.; Cioslowski, J.; Stefanov, B. B.; Liu, G.; Liashenko, A.; Piskorz, P.; Komaromi, I.; Martin, R. L.; Fox, D. J.; Keith, T.; Al-Laham, M. A.; Peng, C. Y.; Nanayakkara, A.; Challacombe, M.; Gill, P. M. W.; Johnson, B.; Chen, W.; Wong, M. W.; Gonzalez, C.; Pople, J. A. *Gaussian 03*, Revision C.02; Gaussian, Inc.: Wallingford, CT, 2004.

(10) Shiragami, T.; Tanaka, K.; Andou, Y.; Tsunami, S.; Matsumoto, J.; Luo, H.; Araki, Y.; Ito, O.; Inoue, H.; Yasuda, M. *J. Photochem. Photobiol., A.* **2005**, *170*, 287.

(11) (a) Marcus, R. A. *Annu. Rev. Phys. Chem.* **1964**, *15*, 144. (b) Marcus, R. A.; Sutin, N. *Biochim. Biophys. Acta* **1985**, *811*, 265. (c) Marcus, R. A. *Angew. Chem., Int. Ed. Engl.* **1993**, *32*, 1111.

(12) (a) Gaines, G. L., III; O'Neil, M. P.; Svec, W. A.; Niemczyk, M. P.; Wasielewski, M. R. *J. Am. Chem. Soc.* **1991**, *113*, 719. (b) Asahi, T.; Ohkohchi, M.; Matsusaka, R.; Mataga, N.; Zhang, R. P.; Osuka, A.; Maruyama, K. *J. Am. Chem. Soc.* **1993**, *115*, 5665. (c) Heitele, H.; Pöllinger, F.; Häberle, T.; Michel-Beyerle, M. E.; Staab, H. A. *J. Phys. Chem.* **1994**, *98*, 7402. (d) DeGraziano, J. M.; Liddell, P. A.; Legett, L.; Moore, A. L.; Moore, T. A.; Gust, D. *J. Phys. Chem.* **1994**, *98*, 1758. (e) Häberle, T.; Hirsh, J.; Pöllinger, F.; Heitele, H.; Michel-Beyerle, M. E.; Anders, C.; Döhling, A.; Krieger, C.; Rückemann, A.; Staab, H. A. *J. Phys. Chem.* **1996**, *100*, 18269. (f) Osuka, A.; Noya, G.; Taniguchi, S.; Okada, T.; Nishimura, Y.; Yamazaki, I.; Mataga, N. *Chem. Eur. J.* **2000**, *6*, 33.